Pertanika J. Sci. & Technol. 27 (S1): 123 - 135 (2019)

PERTANIKA JOURNALS

SCIENCE & TECHNOLOGY

Journal homepage: http://www.pertanika.upm.edu.my/

Mapping the Distribution of Oil Palm using Landsat 8 Data by Comparing Machine Learning and Non-Machine Learning Algorithms

Nur Shafira Nisa Shaharum[1], Helmi Zulhaidi Mohd Shafri[1]*, Wan Azlina Wan Ab Karim Ghani[2], Sheila Samsatli[3] and Badronnisa Yusuf[1]

[1]Department of Civil Engineering /Geospatial Information Science Research Centre (GISRC), Faculty of Engineering, Universiti Putra Malaysia, 43400 UPM Serdang, Selangor, Malaysia.
[2]Department of Chemical and Environmental Engineering/Sustainable Process Engineering Research Centre (SPERC), Faculty of Engineering, Universiti Putra Malaysia, 43400, UPM Serdang, Selangor, Malaysia.
[3]Department of Chemical Engineering, University of Bath, Claverton Down, BA2 7AY, United Kingdom.

ABSTRACT

Oil palm is one of the major crops in Malaysia; it accounts for 47% of the global palm oil supply. Equatorial climate has provided Malaysia with the potential to produce oil palm biomass, which is one of the major contributors to the local economy. The utilisation of oil palm biomass as a source of renewable energy is one of the effective methods to promote green energy. Therefore, there is a need to have sufficient data related to oil palm biomass such as yield estimation, oil palm distributions, and locations. The aim of this study was to produce a land cover map on the distribution of oil palm plantations on three districts located in Selangor. Landsat 8 images of resolutions 15 x 15 m were used and classified via machine learning and non-machine learning algorithms. In this study, three different classifier algorithms were compared using support vector machines, artificial neural networks, and maximum likelihood classifications in which the values obtained for overall accuracy were 98.96%, 99.39%, and 15.30% respectively. The output showed that machine learning algorithms, support vector machines and

ARTICLE INFO

Article history:
Received: 24 October 2018
Accepted:15 February 2019
Published: 21 June 2019

E-mail addresses:
fieranisa94@gmail.com (Nur Shafira Nisa Shaharum)
helmi@upm.edu.my (Helmi Zulhaidi Mohd Shafri)
wanazlina@upm.edu.my (Wan Azlina Wan Ab Karim Ghani)
S.M.C.Samsatli@bath.ac.uk (Sheila Samsatli)
nisa@upm.edu.my (Badronnisa Yusuf)
* Corresponding author

ISSN: 0128-7680
e-ISSN: 2231-8526

artificial neural networks gave rise to high accuracies. Hence, the mapping of oil palm distributions via machine learning algorithm was better than that via non-machine learning algorithm.

Keywords: Landsat 8, machine learning, oil palm, remote sensing, support vector machine

INTRODUCTION

Malaysia is blessed with plenty of biomass crops such as paddy, rubber, and oil palm. In fact, Malaysia is currently one of the largest suppliers of palm oil in the world. As a tropical country that experiences both hot and humid weather, oil palm can be grown over a large area; this in turns bring forth benefits to the local economy in terms of increase in oil palm cultivation (Ng et al., 2012; Sumathi et al., 2008 ; Yusoff, 2006). In 2011, 4.98 Mha of oil palm was grown in Malaysia, and this figure rose to 5.64 Mha in 2016, an increment of 13.25% in 5 years (Malaysian Palm Oil Board, 2016). The aforementioned area is expected to increase over time, and this enhances the feasibility of oil palm as a renewable source of energy (Awalludin et al., 2015).

Globally, the demand for biomass is growing. The development of the oil palm biomass industry in Malaysia needs to be monitored while the role of oil palm biomass as a source of renewable energy requires evaluation (Ng et al., 2012). Biomass is an important alternative to fossil fuels in the production of electricity. Without proper adoption of biomass as a source of renewable energy, Malaysia is likely to contend with an energy crisis in the future (Chuah et al., 2006). In order to fully optimise the local usage of oil palm biomass, detailed information of the distribution of oil palm is vital.

Remote sensing can provide a large area's worth of information from a distance. Data is obtained from the energy that is reflected from the surface of the Earth. A few studies on oil palm mapping have employed various sensors and techniques (Chong et al, 2017; Koh et al., 2011; Nooni et al., 2014). For example, Landsat 7 has been used to map the distribution of oil palm in Selangor via the Nearest Neighbour (NNB) technique, for which the overall accuracy of the results was 98%. However, the image obtained from Landsat 7 was covered with clouds and the map produced was for 2002 (Wahid et al., 2005). Cheng et al. (2017) had utilised MODIS and ALOS Phased Array type L-band Synthetic Aperture Radar mosaiced data via different approaches to map the distribution of oil palm. According to Li et al. (2015), support vector machine is found to be the best classifier to map oil palm using PALSAR data with 50 m spatial resolution. The uses of support vector machines and artificial neural networks for crops classifications give good results (Peña et al., 2014). However, the algorithms need to be tested in order to produce an updated map of oil palm distributions. In this study, Landsat 8 data of spatial resolution 15 x 15 m was used to map the distributions of oil palm. Due to the richness of oil palm area in Selangor, Ahmed et al. (2010) had conducted a study on land cover mapping using Quick Bird and

Sentinel 1 data. Therefore, 3 districts within Selangor were chosen for this study, namely Klang, Petaling, and Kuala Langat. In order to identify the best algorithm for oil palm mapping, maximum likelihood classifier, support vector machines, and artificial neural networks were compared in this study.

MATERIALS AND METHODS

Data which was taken by Landsat 8 Operational Land Imager (OLI) on 29th March 2016 was used in this study. The image shown in Figure 1 has 5.63% of cloud cover and the image was acquired at https://libra.developmentseed.org/. It covered the entire area of Selangor, and was composed of many pixels, each of which was assigned a certain value called Digital Number (DN). The image comprised 11 bands (including Multispectral, Thermal Infrared, Panchromatic, and Cirrus) whose spatial resolutions ranged from 15 x 15 m to 100 x 100 m. In this study, only Multispectral and Panchromatic bands were used, while the areas of interest were the three aforementioned districts (Klang, Petaling, and Kuala Langat). Figure 2 shows the workflow of the study.

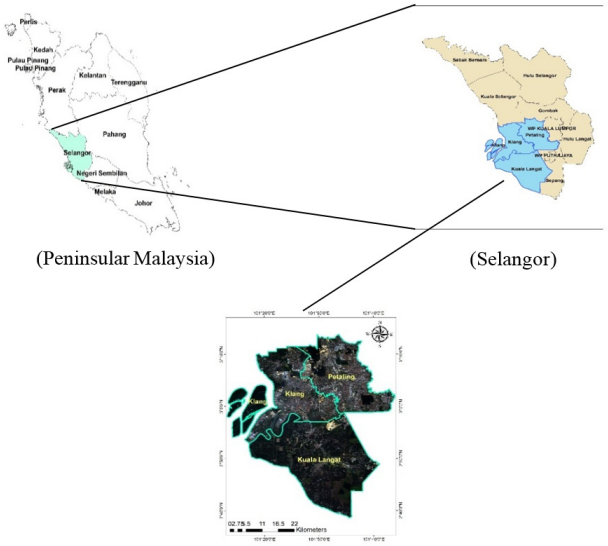

(Klang, Kuala Langat, and Petaling districts as captured by Landsat 8)

Figure 1. Study area covering the three districts

Image Processing

Pre-processing was applied and conducted in ENVI software version 5.3 (ITT Visual Information Solutions, Boulder, CO, USA). A Radiometric Calibration tool was used to correct the raw image of Landsat 8 by converting the DN to reflectance. Multispectral bands contain various number of bands including red, green, blue, and near-infrared with

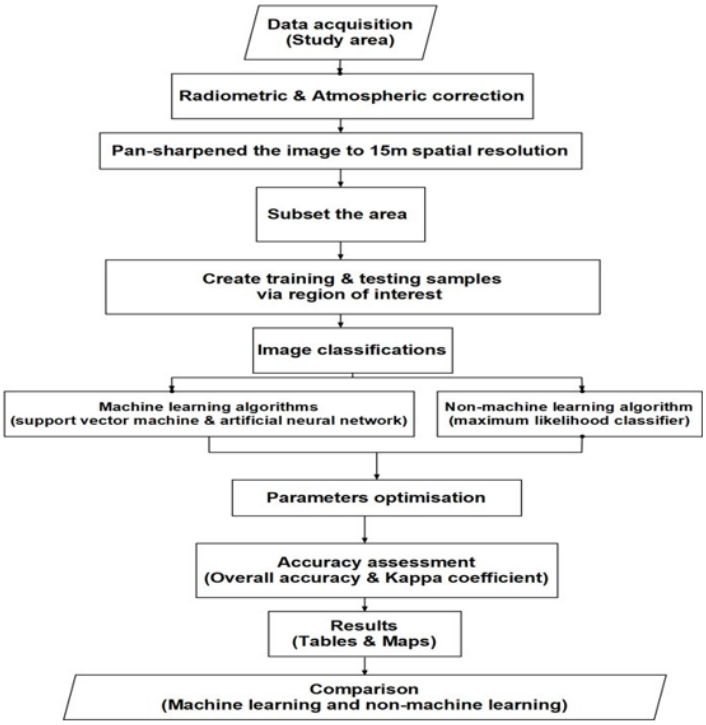

Figure 2. Work flow of the study

the spatial resolution of 30 x 30m. By combining three different bands, it can produce an image with colours. For Landsat 8, a combination of band 4 (Red), band 3 (Green), and band 2 (Blue) will produce an image with true colours shown in Figure 3. On the other hand, panchromatic band is based on higher spatial resolution with 15 x 15m. Following atmospherical correction of the image, an image pan-sharpening technique was employed to increase the spatial resolution from 30 x 30m to 15 x 15 m (Gilbertson et al., 2017; Shaharum et al.,2018). Subsequently, the image was cropped (subset) using the region of interest (ROI) tool in ENVI, leaving only the areas of interest. In addition, the training and testing samples were created using the same ROI tool, with high-resolution images from Google Earth as the reference. The samples were created and labelled according to their classes: oil palm, non-oil palm, bare soil, built-up areas, and water. After that, the image was classified by support vector machines, artificial neural networks, and maximum likelihood classifications. The study area and the placement of the training samples were shown in Figure 3 and Figure 4.

Support Vector Machines

A support vector machine (SVM) is an advanced classifier and one of the powerful machine

Figure 3. True colour of the study area

Figure 4. The samples are placed on the pixels according to the assigned classes

learning algorithms that has been widely used to classify remote sensing images (Shafri, 2016). SVM, which was introduced by Vapnik et al. (1995) is a technique which involves regressions and classifications (Shafri & Ramle, 2009). In light of its high-performance generalisations without the need for prior knowledge, SVM has the ability to produce outstanding results in various applications (Hermes et al., 1999; Kavzoglu & Colkesen, 2009; Shafri & Zeen, 2011; Shafri, 2016). In addition, SVM works by mapping or grouping the data in a high dimensional feature space; this allows the non-linear data points to be separated into the desired classes. Using a hyperplane, SVM separates the support vectors by maximising the distance between the support vectors of each class. In ENVI, four types of kernels are available for SVM: linear, polynomial, radial basis function (RBF), and sigmoid. RBF was chosen for in this study in view of its good performance in previous studies (Kuo et al., 2014; Feizizadeh et al., 2017).

Artificial Neural Networks

Apart from SVM, artificial neural networks (ANNs) are another type of non-parametric machine learning algorithm. The method by which ANN processes information is slightly different from those of other machine learning algorithms such as Decision Tree (DT) and Random Forest (RF). Unlike ANN, DT and RF use a tree-like form to perform classifications (Dibs et al., 2017; Pal, 2005). However, ANN imitates the way by which a human brain processes information (Braga et al., 2016). In the latter, billions of interconnected neurons allow humans to learn and recognise a variety of input pattern. A neuron is made up of a cell body, a longer thread axon, and many fine threads (dendrites), of all which enable the

neurons to send and receive impulses in a human brain. As a result, the brain is capable of learning, predicting, and recognising patterns with ease (Agatonovic-Kustrin & Beresford, 2000; Kumar et al., 2015; Wang et al., 2015).

To produce the structure of biological neurons in a computational design, ANN has been structured in terms of input, hidden, and output layers. Each layer can consist of one or several neurons called nodes. These nodes are connected, with each connection being assigned a certain weight that can be adjusted during the back-propagation method. From the input layer, information is fed onwards to the hidden layer and finally the output layer. An activation function occurs at the nodes when the value from previous node is added to the weight. Theoretically, back-propagation takes place when a signal is sent back to the input layer and again to the output layer. Throughout the process, the weights are adjusted using the provided training samples to minimise errors between the output and actual values. This adjustment process continues until a desired number of iterations is attained (Wang et al., 2015; Shi et al., 2017).

Maximum Likelihood Classifier

A maximum likelihood classifier (MLC) is a non-machine learning algorithm and is the most popular supervised parametric classifier in the field of remote sensing. It works by making assumptions of the probability that a pixel belongs to a certain class. Theoretically, MLC assumes that the probabilities are the same for all classes under the basis that the input bands are normally distributed (Gómez et al., 2016; Rawat & Kumar, 2015).

$$g_i(x) = 1np(\omega_i) - {}^1\!/_2\, 1n|\Sigma_i| - {}^1\!/_2\, (x - m_i)^T \sum_i^{-1} (x - m_i) \qquad (1)$$

Class, i ; n-dimensional data (where n is the number of bands), x; Probability that class ω_i occurs in the image and is assumed the same for all classes, $p(\omega_i)$; Determinant of the covariance matrix of the data in class ω_i, $|\Sigma_i|$; Its inverse matrix, Σ_i^{-1}; Mean vector, m_i

Furthermore, MLC assigns each pixel to the class that has the highest probability. If the highest probability is lower than the specified threshold, the pixel will not be classified. Unlike SVM and ANN, MLC needs prior knowledge. However, the usage decision boundaries by MLC can lead to poor quality results for land cover classifications of large areas (Hubert-Moy et al., 2001).

Parameters Optimisation

Owing to the flexibility of machine learning algorithms, parameters of the algorithms can be tuned to improve the accuracy (Li et al., 2015; Mountrakis et al., 2011). Since no studies had optimised the parameters for mapping oil palm distributions, the parameters in SVM, ANN, and MLC were optimised in this study to improve the classifications using automated approach via python programming language and non-auto parameter tuning in ENVI.

Accuracy Assessment

The accuracy assessment in this study was calculated using confusion matrix provided in ENVI. It produces an error matrix where an overall accuracy and kappa coefficient were given which allow the accuracy of the maps generated to be compared. The overall accuracy is calculated by adding the number of correctly classified values and divide it by the total number of values while kappa coefficient measures the agreement between classification and truth values. Kappa value is ranging from 1 to 0 where the value of 1 represents perfect agreement, while a value of 0 represents no agreement. Example for the calculation of overall accuracy and the kappa coefficient formula were computed as follows:

Overall accuracy = [(13098+296+80+504+1388)/15519] x 100 = 99.01%

$$K = \frac{N\sum_{i=1}^{n} m_{i,i} - \sum_{i=1}^{n}(G_i C_i)}{N^2 - \sum_{i=1}^{n}(G_i C_i)} \quad (2)$$

The class number, i; The total number of classified values compared to truth values, N; The number of values belonging to the truth class i that has also been classified as class i , $m_{i,\,i}$; The total number of predicted values belonging to class i, C_i; The total number of truth values belonging to class i, G_i

In the example confusion matrix, the kappa coefficient is 0.9644

RESULTS AND DISCUSSIONS

Three classifiers were used to classify the image, and the resultant images of each are shown in Figure 5(a), Figure 5(b), and Figure 5(c).

The images in Figure 5 were classified using the same pixel-based technique. Each pixel was 15 m in length and width. With reference to these images, it can be inferred that machine learning algorithms, like SVM and ANN provided good quality classifications in which the parameters were tested and optimised. The best results from the optimised parameters were used to classify the maps. However, a non-machine learning algorithm, MLC gave rise to the worst classification as the overall accuracy of the same was a mere 15.30% (Table 2).

As per the confusion matrix table generated in ENVI, SVM produced an image with producer's and user's accuracies of 92.74% and 89.35% respectively for oil palm. Meanwhile, the said values for ANN were 99.67% and 100% respectively. ANN produced results of better accuracies than SVM. Though ANN produced higher overall accuracy than SVM, the visualisation of the classified map generated by SVM reflected the closest to the satellite image. On the other hand, owing to the misclassification of water as built-up, the map produced by MLC had an excess of built-up areas, which directly affected the overall accuracy. The example of confusion matrix is tabulated in Table 1.

With reference to Table 2, SVM and ANN classified images with high accuracy, this showing that machine learning algorithms performed better than non-machine learning. The overall accuracies of the images produced by SVM and ANN exceeded 98%. In light of the fact that non-parametric algorithms do not make any assumptions, they can easily learn the functional forms of the training data (Ruiz et al., 2014). Also, machine learning algorithms have been proven to be more intelligent than non-machine learning ones owing to their generality and flexibility in fitting many functional forms (Lary et al., 2016; Shafri, 2016).

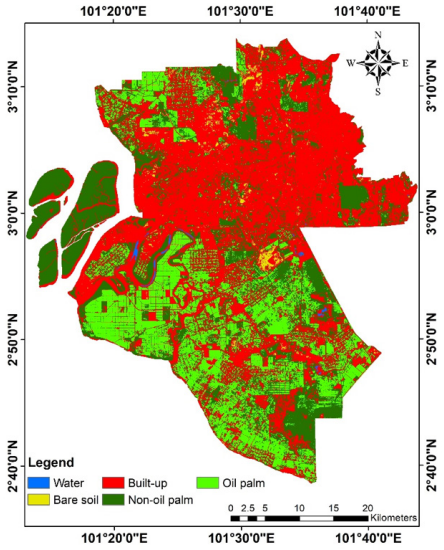

Figure 5(a). Result of maximum likelihood classifierz

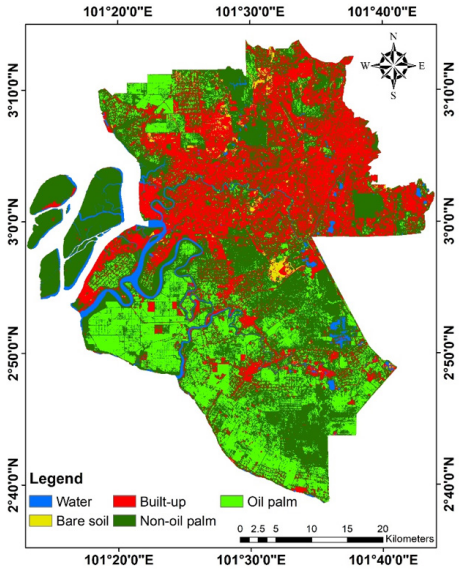

Figure 5(b). Result of support vector machine

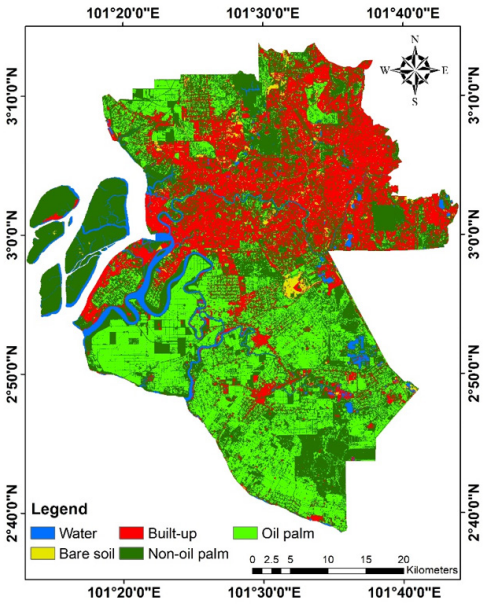

Figure 5(c). Result of artificial neural network

Table 1

Confusion matrix table for a classifier

		Truth				
	Class A	Class B	Class C	Class D	Class E	Total
Class A	13098	0	0	0	5	13103
Class B	0	296	0	0	0	296
Class C	0	6	**80**	0	0	86
Class D	0	0	0	**504**	39	543
Class E	0	1	0	102	**1388**	1491
Total	13098	303	80	606	1432	15519

Predicted

Table 2

Classification results for maximum likelihood classifier, support vector machine, and artificial neural network algorithms

Classifier	Overall accuracy (%)	Kappa coefficient
Maximum likelihood	15.30	0.1297
Support vector machine	98.96	0.9623
Artificial neural network	99.39	0.9779

McNemar's Test

McNemar's test is a statistical test which employs a 2 x 2 matrix to compare the significance of the difference between two methods. Usually, a significance level of 95% is used, for which a test is said to be statistically significant when $\rho \leq 0.05$. As per Table 2, the accuracies of the images produced by SVM and ANN were relatively close to each other. Subsequently, McNemar's test was done to compare the results between ANN and SVM. A ρ-value of 0.06 was obtained, while the chi-square (x^2) was calculated as follows:

$$\chi^2 = \frac{(b-c)^2}{b+c} \quad (3)$$

Number of samples that were correctly identified by classifier 1 but wrongly classified by classifier 2, *b*; Number of samples that were wrongly classified by classifier 1 but correctly classified by classifier 2, *c*

The value of x^2 was 3.50 for 1 degree of freedom. Since the value was less than 3.84, the hypothesis that there was no association between the training samples and classifiers was accepted and as the model befitted the data. Also, the absence of a statistically significant association was also in light of the fact that the calculated ρ-value was greater than 0.05.

CONCLUSION

The main objective of this study is to measure the effectiveness of machine learning and non-machine learning algorithms on land cover mapping. With a slight difference of less than 0.5%, the results produced by SVM and ANN were considered to be comparable. Furthermore, these machine learning algorithms are capable of improving the accuracy of the map produced by optimising the desired parameters. In terms of overall accuracy, both aforementioned machine learning algorithms outperformed the non-machine learning parametric classifier, MLC by more than 83%. The effectiveness of machine learning algorithms in classifying the land cover − including the oil palm plantations − of the three districts was promising. The said gap has shown that machine learning was a powerful and an advanced algorithm that worked better than non-machine learning algorithms in the classification of images. The ability to produce highly accurate results with a limited number of training samples was an advantage of SVM. In addition, SVM is much easier to optimise the parameters. However, the ability of ANN to work like a human brain and learn from prior experience has led to its production of best overall accuracy result. Generally, areas of oil palm crops can be well-detected by machine learning algorithms. This method can later can be used for further analysis by quantifying information such as areas of biomass crops and estimations of yield for an optimisation and improvement. In conclusion, machine learning algorithms work better with limited training samples and produce better results than non-machine learning algorithms.

ACKNOWLEDGEMENT

The author would like to thank UPM for their facilities and funding of this research. Apart from that, our heartfelt gratitude also goes to Engineering and Physical Sciences Research Council for their financial support through the BEFEW project (Grant No. EP/P018165/1).

REFERENCES

Agatonovic-Kustrin, S., & Beresford, R. (2000). Basic concepts of artificial neural network (ANN) modeling and its application in pharmaceutical research. *Journal of Pharmaceutical and Biomedical Analysis, 22*(5), 717-727.

Ahmed, A. A., Pradhan, B., Sameen, M. I., & Makky, A. M. (2018). An optimized object-based analysis for vegetation mapping using integration of Quickbird and Sentinel-1 data. *Arabian Journal of Geosciences, 11*(11), 1-10.

Awalludin, M. F., Sulaiman, O., Hashim, R., & Nadhari, W. N. A. W. (2015). An overview of the oil palm industry in Malaysia and its waste utilization through thermochemical conversion, specifically via liquefaction. *Renewable and Sustainable Energy Reviews, 50*, 1469-1484.

Braga, J. R. G., Conte, G., Doherty, P., Velho, H. F. C., & Shiguemori, E. H. (2016). Use of artificial neural networks for automatic categorical change detection in satellite imagery. In *4th Conference of Computational Interdisciplinary Sciences* (pp. 1-13). São Paulo, Brazil.

Cheng, Y., Yu, L., Xu, Y., Lu, H., Cracknell, A. P., Kanniah, K., & Gong, P. (2018). Mapping oil palm extent in Malaysia using ALOS-2 PALSAR-2 data. *International Journal of Remote Sensing, 39*(2), 432-452.

Chong, K. L., Kanniah, K. D., Pohl, C. & Tan, K. P. (2017). A review of remote sensing applications for oil palm studies. *Geo-spatial Information Science, 20*(2), 184-200.

Chuah, T. G., Ghani, W. A. W. A. K., Yunus, Robiah., & Omar, R. (2006). Biomass as the renewable energy sources in Malaysia: An overview. *International Journal of Green Energy, 3*(3), 323-346.

Dibs, H., Idrees, M. O., & Alsalhin, G. B. A. (2017). Hierarchical classification approach for mapping rubber tree growth using per-pixel and object-oriented classifiers with SPOT-5 imagery. *The Egyptian Journal of Remote Sensing and Space Science, 20*(1), 21-30.

Feizizadeh, B., Roodposhti, M. S., Blaschke, T., & Aryal, J. (2017). Comparing GIS-based support vector machine kernel functions for landslide susceptibility mapping. *Arabian Journal of Geosciences, 10*(5), 122.

Gilbertson, J. K., Kemp, J., & Van Niekerk, A. (2017). Effect of pan-sharpening multi-temporal Landsat 8 imagery for crop type differentiation using different classification techniques. *Computers and Electronics in Agriculture, 134*, 151-159.

Gómez, C., White, J. C., & Wulder, M. A. (2016). Optical remotely sensed time series data for land cover classification: A review. *ISPRS Journal of Photogrammetry and Remote Sensing, 116*, 55-72.

Hermes, L., Frieauff, D., Puzicha, J. & Buhmann, J. M. (1999). Support vector machines for land usage classification in Landsat TM imagery. In *Proceedings of International Geoscience and Remote Sensing Symposium* (Vol. 1, pp. 348-350). Hamburg, Germany.

Hubert-Moy, L., Cotonnec, A., Le Du, L., Chardin, A., & Perez, P. (2001). A comparison of parametric classification procedures of remotely sensed data applied on different landscape units. *Remote Sensing of Environment, 75*(2), 174-187.

Kavzoglu, T., & Colkesen, I. (2009). A kernel functions analysis for support vector machines for land cover classification. *International Journal of Applied Earth Observation and Geoinformation, 11*(5), 352-359.

Koh, L. P., Miettinen, J., Liew, S. C., & Ghazoul, J. (2011). Remotely sensed evidence of tropical peatland conversion to oil palm. *Proceedings of the National Academy of Sciences, 108*(12), 5127-5132.

Kumar, P., Gupta, D. K., Mishra, V. N., & Prasad, R. (2015). Comparison of support vector machine, artificial neural network, and spectral angle mapper algorithms for crop classification using LISS IV data. *International Journal of Remote Sensing, 36*(6), 1604-1617.

Kuo, B. C., Ho, H. H., Li, C. H., Hung, C. C., & Taur, J. S. (2014). A kernel-based feature selection method for SVM with RBF kernel for hyperspectral image classification. *IEEE Journal of Selected Topics in Applied Earth Observations and Remote Sensing, 7*(1), 317-326.

Lary, D. J., Alavi, A. H., Gandomi, A. H., & Walker, A. L. (2016). Machine learning in geosciences and remote sensing. *Geoscience Frontiers, 7*(1), 3-10.

Li, L., Chen, Y., Xu, T., Liu, R., Shi, K., & Huang, C. (2015). Super-resolution mapping of wetland inundation from remote sensing imagery based on integration of back-propagation neural network and genetic algorithm. *Remote Sensing of Environment, 164*, 142-154.

Li, L., Dong, J., Njeudeng Tenku, S., & Xiao, X. (2015). Mapping oil palm plantations in Cameroon using PALSAR 50-m Orthorectified Mosaic images. *Remote Sensing, 7*(2), 1206-1224.

Mountrakis, G., Im, J., & Ogole, C. (2011). Support vector machines in remote sensing: A review. *ISPRS Journal of Photogrammetry and Remote Sensing, 66*(3), 247-259.

Malaysian Palm Oil Board. (2016). *NKEA Biogas Working Group (BIOGAS WG). NKEA Biogas Working Group Report - Monthly update*. Bangi, Malaysia.

Ng, W. P. Q., Lam, H. L., Ng, F. Y., Kamal, M., & Lim, J. H. E. (2012). Waste-to-wealth: Green potential from palm biomass in Malaysia. *Journal of Cleaner Production, 34*, 57-65.

Nooni, I. K., Duker, A. A., Van Duren, I., Addae-Wireko, L., & Osei Jnr, E. M. (2014). Support vector machine to map oil palm in a heterogeneous environment. *International journal of Remote Sensing, 35*(13), 4778-4794.

Pal, M. (2005). Random forest classifier for remote sensing classification. *International Journal of Remote Sensing, 26*(1), 217-222

Peña, J. M., Gutiérrez, P. A., Hervás-Martínez, C., Six, J., Plant, R. E., & López-Granados, F. (2014). Object-based image classification of summer crops with machine learning methods. *Remote Sensing*, *6*(6), 5019-5041.

Rawat, J. S., & Kumar, M. (2015). Monitoring land use/cover change using remote sensing and GIS techniques: A case study of Hawalbagh block, district Almora, Uttarakhand, India. *The Egyptian Journal of Remote Sensing and Space Science, 18*(1), 77-84.

Ruiz, P., Mateos, J., Camps-Valls, G., Molina, R., & Katsaggelos, A. K. (2014). Bayesian active remote sensing image classification. *IEEE Transactions on Geoscience and Remote Sensing, 52*(4), 2186-2196.

Shaharum, N. S. N., Shafri, H. Z. M., Gambo, J., & Abidin, F. A. Z. (2018). Mapping of Krau Wildlife Reserve (KWR) protected area using landsat 8 and supervised classification algorithms. *Remote Sensing Applications: Society and Environment, 10*, 24-35.

Shafri, H. Z. M., & Ramle, F. S. H. (2009). A comparison of support vector machine and decision tree classifications using satellite data of Langkawi Island. *Information Technology Journal, 8*(1), 64-70.

Shafri, H. Z. M., & Zeen, R. M. (2011). Mapping Malaysian urban environment from airborne hyperspectral sensor system in the VIS-NIR (0.4-1.1 μm) Spectrum. *Research Journal of Environmental Sciences, 5*(6), 587.

Shafri, H. Z. M. (2016). Machine learning in hyperspectral and multispectral remote sensing data analysis. In *Proceedings of the 2016 International Conference* (pp. 3-9). Shanghai, China.

Shi, B., Bai, X., & Yao, C. (2017). An end-to-end trainable neural network for image-based sequence recognition and its application to scene text recognition. *IEEE Transactions on Pattern Analysis and Machine Intelligence, 39*(11), 2298-2304.

Sumathi, S., Chai, S. P., & Mohamed, A. R. (2008). Utilization of oil palm as a source of renewable energy in Malaysia. *Renewable and Sustainable Energy Reviews, 12*(9), 2404-2421.

Vapnik, V., Guyon, I., & Hastie, T. (1995). Support vector machines. *Mach Learn, 20(3),* 273-297.

Wahid, B. O., Nordiana, A. A., & Tarmizi, A. M. (2005). Satellite mapping of oil palm land use. *MPOB Information Series, MPOB TT*, 255, 1511-7871.

Wang, L., Zeng, Y., & Chen, T. (2015). Back propagation neural network with adaptive differential evolution algorithm for time series forecasting. *Expert Systems with Applications, 42*(2), 855-863.

Yusoff, S. (2006). Renewable energy from palm oil–innovation on effective utilization of waste. *Journal of Cleaner Production, 14*(1), 87-93.